

# Key Binding Interactions for Memantine in the *N*-Methyl-*D*-Aspartate Receptor<sup>1</sup>

## 3.1 Introduction

*N*-Methyl-*D*-aspartate (NMDA) receptors are members of the ionotropic glutamate receptor (iGluR) family, which also includes AMPA and kainate receptors (1-3). These are fast, excitatory, ligand-gated ion channels activated by the agonist glutamate and, only in the case of NMDA receptors, a co-agonist such as glycine or *D*-serine (4, 5). The NMDA ion channel is highly permeable to Ca<sup>2+</sup> and is blocked by Mg<sup>2+</sup> in a voltage-dependent manner (1, 6). The NMDA receptor is thought to play a central role in learning and memory and is essential to the normal function of the central nervous system (7, 8). Overactivation of the receptor has been implicated in many neurological disorders, such as Alzheimer's disease, Parkinson's disease, Huntington's disease, amyotrophic lateral sclerosis, schizophrenia, epilepsy, and neurodegeneration following stroke (2, 9–11). Several neuroprotective drugs have been developed to block the NMDA receptor, preventing overactivation. However, most of them cause

---

<sup>1</sup> This work was performed in collaboration with Wesley Yu and Emma Branigan as part of their Summer Undergraduate Research Fellowships at Caltech. A version of this chapter has been submitted for publication.

debilitating side effects due to the critical roles that NMDA receptors play in brain function (12).

Memantine (Namenda<sup>®</sup>) is the unique exception and is currently approved for use in moderate to severe Alzheimer's (13–15). Memantine is thought to function by preferentially blocking open NMDA channels (an uncompetitive antagonist) (16, 17), and hence, a balance between open and closed channels can be achieved by adjusting dosage (12, 14, 18). The interaction between NMDA receptors and memantine is reversible, and the mechanism of block has not been fully elucidated (19).

In this study, we prepared mutants in the pore loop and the third transmembrane (TM3) domain of the GluN1/GluN2B NMDA receptor and measured how these side-chain modifications affect memantine block. Side-by-side comparison of the  $IC_{50}$  for memantine and amantadine (Figure 3.1), a structurally related drug, enabled us to identify the hydrophobic binding pockets for the two methyl groups on memantine. While adding two methyl groups to amantadine to produce memantine improved affinity greatly, we also found that adding a third methyl group to produce the symmetrical trimethylamantadine (TMAM) diminished affinity (Figure 3.1). Our results provide a better understanding of chemical-scale interactions between memantine and the ion pore of NMDA receptor, which will potentially benefit the development of new drugs for neurodegenerative diseases involving NMDA receptors.

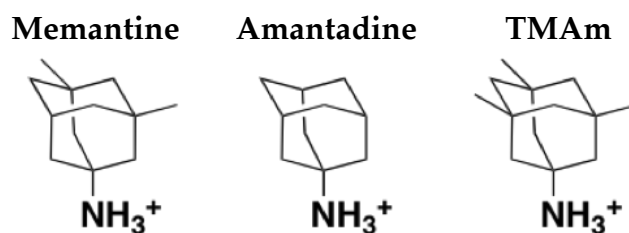


**Figure 3.1.** Structures of memantine, amantadine, and trimethylamantadine (TMAM)

## 3.2 Results

### 3.2.1 Homology models of GluN1 and GluN2B transmembrane domains

The structure of the transmembrane domain of the NMDA receptor is not currently available. It was proposed some time ago that the transmembrane domain of iGluRs is homologous to the pore region of potassium channels, but with the opposite orientation with respect to the membrane (20, 21). This has been confirmed by a crystal structure of a full-length AMPA receptor (22), but unfortunately, the image is of a closed channel and is missing a significant number of residues in the pore loop. Therefore, we created a homology model of GluN1 and GluN2B transmembrane domains, based on the crystal structure of the open-form Kv2.1 paddle-Kv1.2 chimera potassium channel (Protein Data Bank code 2R9R) without any optimization (Figure 3.2) (23).

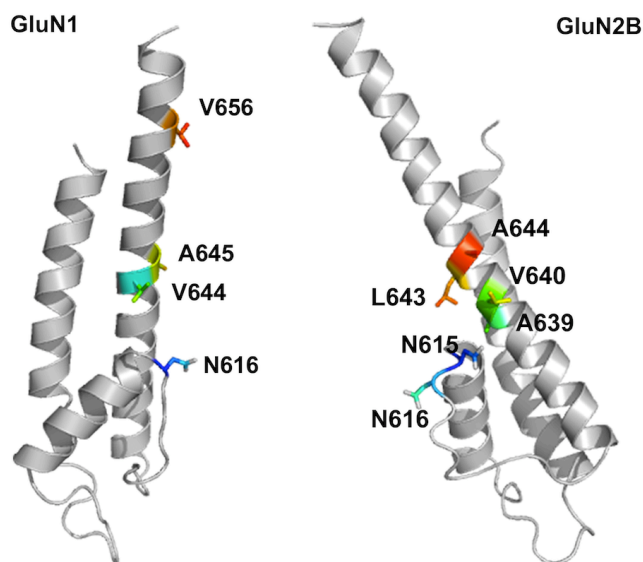


**Figure 3.2.** Homology model of the transmembrane region of GluN1 (*left*) and GluN2B (*right*) subunits of NMDA receptor. The relative position of the two subunits are currently unknown.

### 3.2.2 Mutational scanning

We first performed a mutational scanning on the pore loop, TM3, and post-TM3 regions of the GluN1/2B NMDA receptor using both conventional and unnatural amino acid mutagenesis. Mutations that shift the  $IC_{50}$  greater than 5 folds are deemed significant. The data suggest that no point mutation deeper in the pore than residue GluN1-N616 had a significant effect on memantine blockade, and only mutations at residues V644, A645, and V656 in the TM3/post-TM3 regions of GluN1 had a meaningful impact on the memantine block (Figure 3.3). These preliminary results provided the groundwork for further investigation.

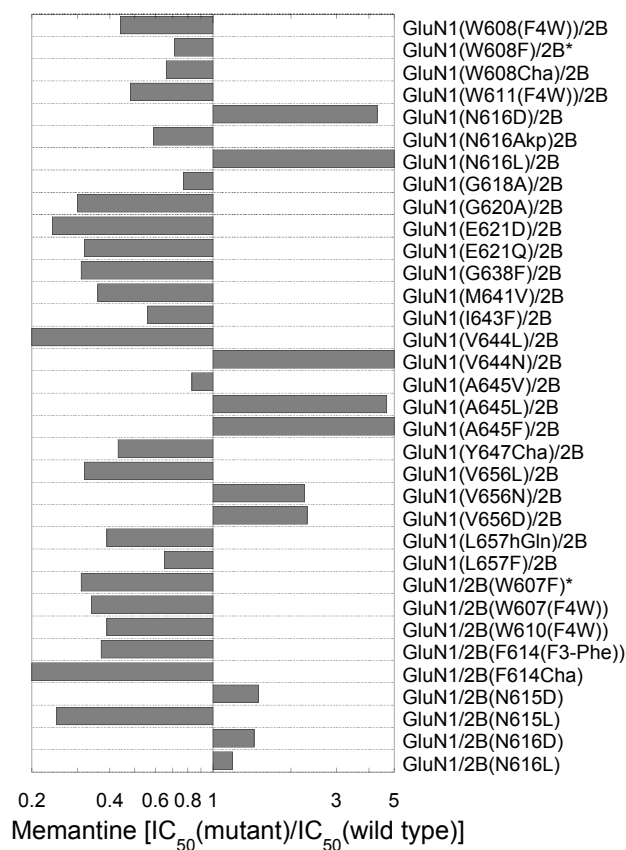


**Figure 3.3.** Memantine fold shifts ( $IC_{50}(\text{mutant})/IC_{50}(\text{wild type})$ ) of mutant NMDA receptors containing a conventional or an unnatural mutation in the transmembrane region. Abbreviation used are F4W, 2,3,4,5-fluoro-Trp; Cha, cyclohexylalanine; hGln, homoglutamine; F3-Phe, 3,4,5-fluoro-Phe. \*, Conventional mutations performed through the nonsense-suppression method.

### 3.2.3 Comparison of memantine and amantadine block

In the present study, we sought to define the scope of the memantine primary binding site by identifying the residues that directly contact the two methyl groups (Figure 3.1). To probe for the methyl group binding pockets of memantine on the NMDA receptor, we considered amantadine, a common antiviral agent that is known to block the channel of NMDA receptors, but with a

lower affinity than memantine (24–30). Amantadine has the same basic core structure as memantine (Figure 3.3), the only difference being that amantadine lacks the two methyl groups present on memantine. Comparing memantine to amantadine, the affinity gained from the presence of the methyl groups is evaluated by  $IC_{50}(\text{amantadine})/IC_{50}(\text{memantine})$ , referred to as the *methyl effect* throughout this chapter. In spite of the small structural difference, the affinity of memantine is 75-fold higher than amantadine in the wild-type receptor (Table 3.3, Figure 3.4), indicating that the two additional methyl groups play an important role in antagonism.

If these two antagonists bind at the same location and orientation in the NMDA channel pore, mutations at residues that interact with the methyl groups are expected to cause a larger  $IC_{50}$  shift for memantine than amantadine, thus, reducing the methyl effect. Smaller methyl effect means the mutant receptor is *less* sensitive toward the methyl group. Other mutations should affect binding of the two antagonists in a similar way. In fact, memantine and amantadine show similar responses to the GluN1(N616Q) and the GluN1(N616D) mutations (Figure 3.4) — a residue that is thought to anchor the ammonium group through an electrostatic interaction (12, 31). Mutations at the analogous residues in GluN2, N615D and N616D, produce relatively modest effects (Figure 3.4). The GluN2(N615D) mutation is unique in that it affects amantadine binding more than memantine. All the data are consistent with the notion that the two drugs block the channel at the same general location.

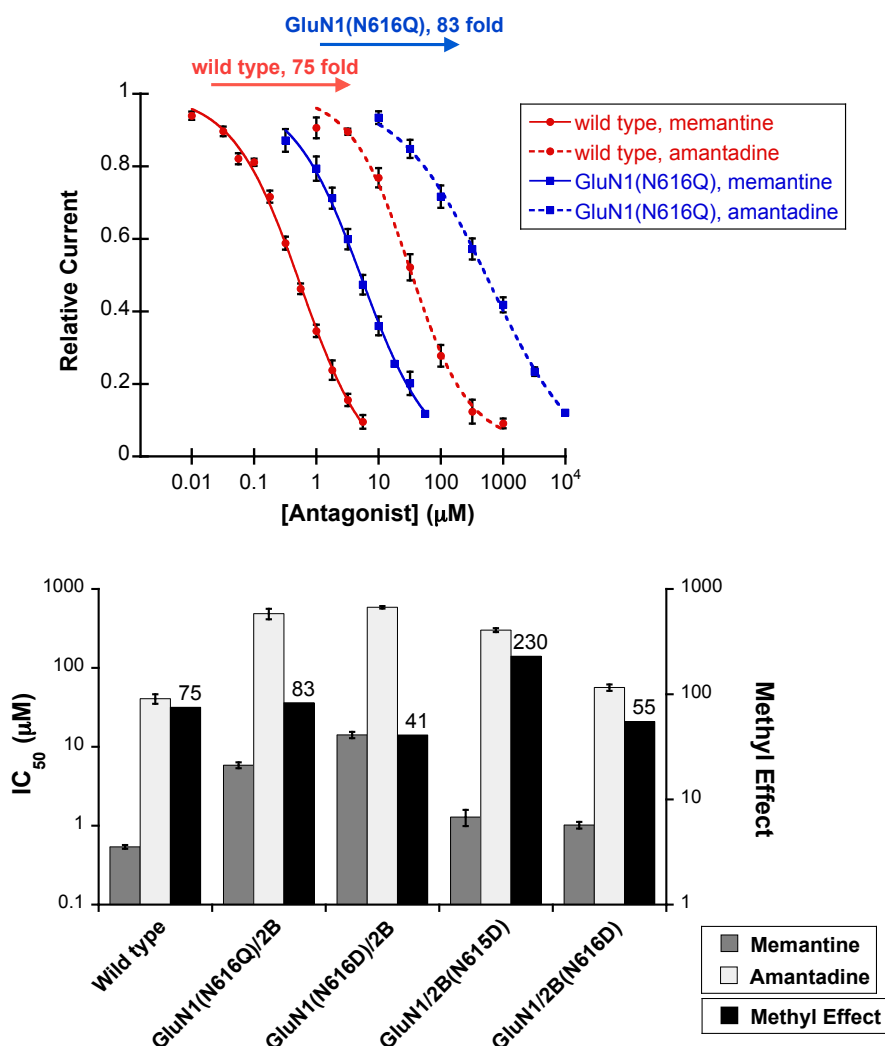


**Figure 3.4.** Memantine and amantadine dose response curves for the wild-type and the GluN1(N616Q) mutant NMDA receptors (*top*). The respective methyl effects are shown above the curves. Memantine IC<sub>50</sub>, amantadine IC<sub>50</sub>, and the methyl effect for wild-type and mutant NMDA receptors containing a mutation at GluN1-N616, GluN2B-N615, or GluN2B-N616 (*bottom*). The values for IC<sub>50</sub> ± s.e.m. are shown in Table 3.3. The methyl effect values are shown above the corresponding columns.

### 3.3.4 Mapping the methyl group binding site on GluN1

Since we are probing for a hydrophobic binding pocket for the methyl groups, our strategy was to make hydrophobic side chains more hydrophilic.

Therefore, we mutated these three residues to Asn. The impact of mutations in the GluN1 subunit on  $IC_{50}$  values of both memantine and amantadine are shown in Figure 3.5 and Table 3.3.

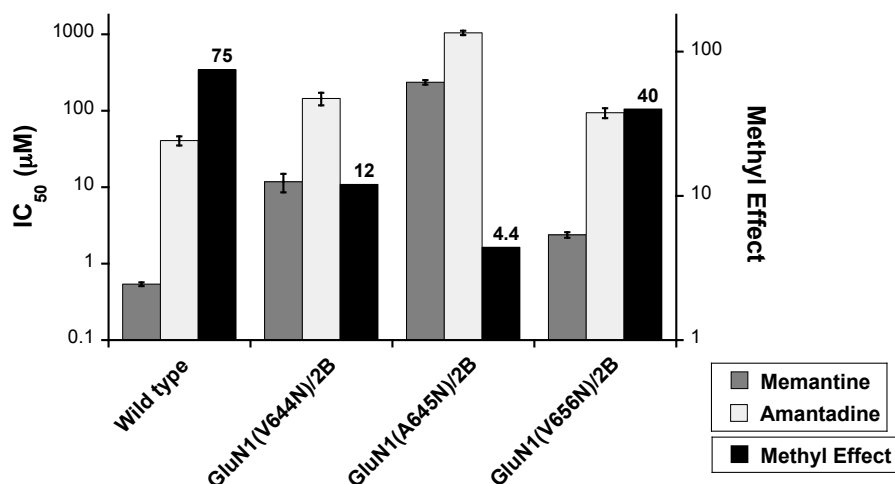


**Figure 3.5.** Memantine  $IC_{50}$ , amantadine  $IC_{50}$ , and the methyl effect for wild-type and mutant NMDA receptors containing a mutation at the residue V644, A645, or V656 in GluN1. The values for  $IC_{50} \pm$  s.e.m. are shown in Table 3.3. The methyl effect values are shown above the corresponding columns.

The mutation V644N impacted the binding of memantine significantly more than amantadine. The  $IC_{50}$  ratio between the two drugs decreased to 12-fold, compared to the 75-fold effect seen in the wild-type receptor (Figure 3.5). The adjacent A645N mutation showed an even larger effect, with only a 4.4-fold difference between memantine and amantadine  $IC_{50}$ . The mutation V656N causes only a moderate 4.4-fold shift in  $IC_{50}$  for memantine and a modest 2.3-fold shift for amantadine. Interestingly, this mutation causes a nearly 10-fold shift in glutamate  $EC_{50}$  (Table 3.1), which may imply a strong perturbation to receptor gating.

Although the effects of Asn mutations at GluN1 residue 644 and 645 on glutamate  $EC_{50}$  were much smaller than the effects on blockage, the A645N mutation did show the significant reduction in Glu  $EC_{50}$ , approximately 6-fold (Table 3.1). In order to determine whether the V644N and A645N data in Figure 3.5 resulted from an unwanted structural perturbation, we tested V644T, V644L, A645V, and A645L mutations. All of these mutations shift glutamate  $EC_{50}$  less than A645N (Table 3.1). The additional mutations at residue 644 did not have a considerable impact on memantine  $IC_{50}$ , amantadine  $IC_{50}$ , or the ratio between the two (Table 3.3). Neither did the Val mutation at residue 645 (Figure 3.6, Table 3.3). In contrast, the A645L mutation had a significant impact on memantine  $IC_{50}$ , while essentially no effect is seen with amantadine  $IC_{50}$  (Figure 3.6, Table 3.3).

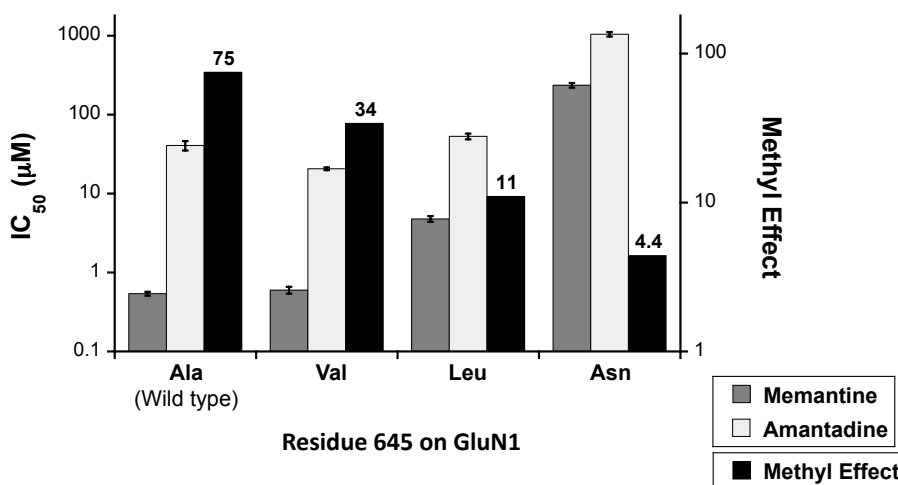


**Figure 3.6.** Memantine  $IC_{50}$ , amantadine  $IC_{50}$ , and the methyl effect for wild-type and mutant NMDA receptors containing a mutation at the residue GluN1-A645. The values for  $IC_{50} \pm$  s.e.m. are shown in Table 3.3. The methyl effect values are shown above the corresponding columns.

A trend is seen in which the methyl effect is reduced with increasing the side-chain volume (Ala > Val > Leu) and side-chain polarity (Leu > Asn) at residue 645 (Figure 3.6). These results suggest that the residue A645 on GluN1 contributes to the methyl group binding site of memantine, while the residue V644 is located in close proximity.

### 3.3.5 Mapping the methyl group binding site on GluN2

Models of the NMDA receptor heterotetramer indicate that both GluN1 and GluN2 contribute to the channel region being probed. To probe for contributions to a methyl group binding site by GluN2B, however, it is not safe to assume that the residue GluN2-A644, which would typically be considered to align with GluN1-A645 (21, 32), also contributes to a methyl group binding site. A previous study by the substituted cysteine accessibility method (SCAM) on GluN1/GluN2C suggests that there may be an offset by four residues in the TM3 regions between the GluN1 and GluN2C (21, 32, 33). Accordingly, we considered the aligning residues, L643 and A644, as well as the residues A639 and V640 which are one helix turn lower in the structure (Figure 3.2). The A639N and V640N mutations had a negligible effect on memantine and amantadine binding (Figure 3.7). In contrast, L643N and A644N substantially impaired memantine blockade. Similar to what is seen with GluN1, GluN2(L643N) shows a modest differentiation between memantine and amantadine, while GluN2(A644N) shows a quite substantial effect (Figure 3.7).

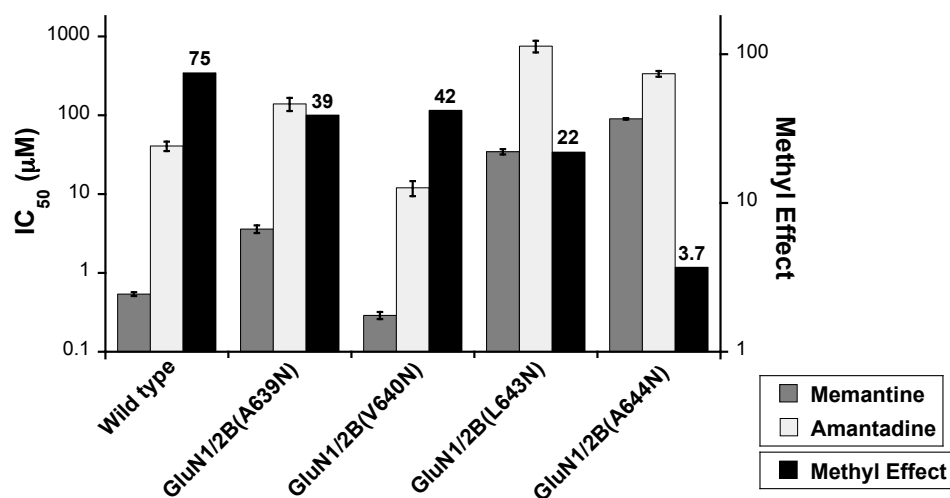


**Figure 3.7.** Memantine IC<sub>50</sub>, amantadine IC<sub>50</sub>, and the methyl effect for wild-type and mutant NMDA receptors containing an Asn mutation at the residue A639, A640, L643, and A644 in GluN2B. The values for IC<sub>50</sub> ± s.e.m. are shown in Table 3.3. The methyl effect values are shown above the corresponding columns.

Parallel to the study in GluN1 subunit, we also mutated GluN2-A644 to the hydrophobic side chains Leu and Val. All these mutations resulted in minimal changes to glutamate EC<sub>50</sub> (Table 3.1). Adding volume to this side chain (Ala > Val > Leu) lowered amantadine IC<sub>50</sub> while leaving the memantine IC<sub>50</sub> unaltered (Figure 3.8). Thus, the trend in the methyl effects is similar to that seen for mutations at GluN1-A645, in which there is a reduction in the methyl effect as the side-chain volume or the side-chain polarity is increased (Figure 3.8). Overall, these results suggest these two residues — GluN1-A645 and GluN2-A644 — play similar roles in shaping the memantine methyl binding site.

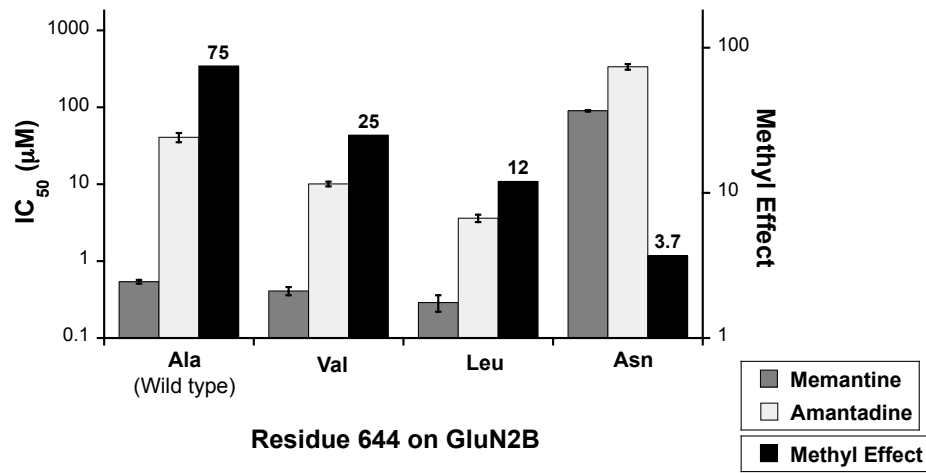


**Figure 3.8.** Memantine IC<sub>50</sub>, amantadine IC<sub>50</sub>, and the methyl effect for wild-type and mutant NMDA receptors containing a mutation at the residue GluN2B-A644. The values for IC<sub>50</sub> ± s.e.m. are shown in Table 3.3. The methyl effect values are shown above the corresponding columns.

**Table 3.1.** Glutamate EC<sub>50</sub> ± s.e.m. and Hill constant of wild-type and mutant NMDA receptors

NMDA Receptor	Glutamate EC <sub>50</sub>	Hill Constant	<i>n</i>	EC <sub>50</sub> (mutant)/EC <sub>50</sub> (wild type)
	μM			
Wild type	1.94 ± 0.04	1.7	8	1.00
<b>GluN1 Mutants</b>				
N616Q	0.47 ± 0.01	1.6	11	0.24
N616D	1.3 ± 0.02	1.8	14	0.65
V644T	2.0 ± 0.03	1.6	11	1.01
V644L	1.3 ± 0.02	1.5	10	0.67
V644N	1.7 ± 0.03	1.6	12	0.89
A645V	0.93 ± 0.03	1.6	8	0.48
A645L	0.60 ± 0.02	1.3	9	0.31
A645N	0.33 ± 0.01	2.1	7	0.17
V656N	0.20 ± 0.01	2.3	7	0.10
<b>GluN2B Mutants</b>				
N615D	2.9 ± 0.06	1.7	5	1.01
N616D	2.8 ± 0.04	1.5	6	1.45
A639N	0.63 ± 0.02	1.5	9	0.32
V640N	2.8 ± 0.10	1.6	9	1.42
L643N	1.2 ± 0.03	1.5	9	0.64
A644V	0.61 ± 0.05	1.2	5	0.31
A644L	0.76 ± 0.05	1.5	11	0.39
A644N	0.73 ± 0.01	1.7	9	0.37

### 3.3.6 Investigating trimethylamantadine blockade

To further probe the possible role of methyl groups and asymmetry in the binding region, we considered the molecule trimethylamantadine (TMAM, Figure 3.1). The additional methyl group of TMAM introduces a 3-fold rotation axis that is absent in memantine. We found that this molecule blocks the NMDA receptor with an  $IC_{50}$  of 3.4  $\mu$ M (Table 3.2), intermediate between the values for memantine (0.54  $\mu$ M) and amantadine (41  $\mu$ M). However, the GluN1(N616Q) mutation that displays a substantial shift in both memantine and amantadine  $IC_{50}$  does not have any effect on TMAM block (Table 3.2). Similarly, Asp mutation at GluN2-N615 or GluN2-N616 do not shift the TMAM  $IC_{50}$  from the wild-type value. TMAM is sensitive to GluN1(A645N) and GluN2(A644N) mutations, but the mutations have a significantly smaller effect on  $IC_{50}$  shifts for TMAM compared to memantine. These data imply that the TMAM molecule interacts with the ion pore in a different orientation than memantine and amantadine.

**Table 3.2.** TMAM  $IC_{50} \pm$  s.e.m. for wild-type and mutant NMDA receptors

NMDA Receptor	TMAM $IC_{50}$	$n$	$IC_{50}(\text{mutant})/IC_{50}(\text{wild type})$
	$\mu$ M		
Wild type	3.4 $\pm$ 0.4	10	1.0
GluN1(N616Q)/2B	2.0 $\pm$ 0.08	9	0.6
GluN1(V644T)/2B	3.1 $\pm$ 0.4	10	0.9
GluN1(A645N)/2B	180 $\pm$ 11	12	53
GluN1/2B(N615D)	5.4 $\pm$ 1.1	13	1.6
GluN1/2B(N616D)	2.9 $\pm$ 0.4	8	0.9
GluN1/2B(V640N)	0.72 $\pm$ 0.1	8	0.2
GluN1/2B(A644N)	100 $\pm$ 7.4	11	30

### 3.3 Discussion

Memantine is currently prescribed as a treatment for moderate to severe Alzheimer's disease (13-15), and the drug also displays clinical potential for treatment of other neurodegenerative disorders (18, 34, 35). Memantine is believed to function by blocking the NMDA receptor, a glutamate-gated ion channel in the brain, but the key binding interactions between drug and receptor are not fully elucidated (16, 17, 19). Further understanding of the chemical-scale interactions between the NMDA receptor and memantine will contribute some insight into the detailed mechanism of memantine blockade that underlies its high clinical potential.

Previous studies suggested that memantine can block the NMDA receptor at multiple sites, and the primary binding site (the one with the highest affinity or lowest  $IC_{50}$ ) involves an interaction between the ammonium group of memantine and the side chain of an Asn residue (residue 616, the N/Q site) in the GluN1 subunit (Figure 3.2) (12, 31). This residue is located at the tip of the pore loop, which forms the narrowest constriction of the NMDA pore (1, 20, 21). Our preliminary mutational scanning results suggest that no point mutation deeper in the pore than residue Asn616 had a significant effect on memantine blockade (Figure 3.3), consistent with a previous report that memantine cannot block NMDA receptors from the intracellular site (36). Furthermore, Kashiwagi et al. previously suggested that mutations at residues on the TM3 and post-TM3 regions of GluN1 had a considerable impact on memantine  $IC_{50}$ s (37). When we map these residues onto our homology model (Figure 3.2), we found some of

them to be distant from the Asn residue that anchors the ammonium of memantine. It seemed very unlikely that a small molecule like memantine would interact directly with all these residues. For these reasons, we aimed to search for the methyl group binding pockets that would serve as the definite upper boundary of the memantine primary binding site.

The highest memantine concentration used in all IC<sub>50</sub> experiments was 100 μM to minimize complications involving the secondary (lower affinity) binding site (12, 29, 30, 38) and/or antagonist trapping (27, 39, 40). Though this choice prevented completion of full dose-response curves for some mutations, meaningful IC<sub>50</sub> values (unlike EC<sub>50</sub> values) can be obtained from such plots. The EC<sub>50</sub> for glutamate was measured for all the mutant receptors to ensure that (i) the mutant receptors are functional and (ii) a saturating dose of glutamate (4 or 10 μM) was applied to activate the mutant receptors in the IC<sub>50</sub> experiments (Table 3.1).

In order to identify the residues that interact with the methyl groups, we employed a structurally related NMDA antagonist, amantadine, from which the methyl groups are absent. Mutations at the residues in contact with the methyl groups should have a larger effect on memantine affinity than amantadine, while other mutations should have a comparable effect on the two antagonists.

Probing wild-type vs. a mutant receptor with two different antagonists sets up an opportunity for a mutant cycle analysis as a way to evaluate meaningful interactions. The basic scheme is shown in Figure 3.9. The coupling parameter defines the deviation from additivity of the two “mutations”: the change to the receptor and the removal of the methyl groups of memantine to

make amantadine. Significant coupling suggests an important interaction between the protein side chain being mutated and the methyl groups. The coupling parameter,  $\Omega$ , can be converted to a free energy by the equation  $\Delta\Delta G^\circ = -RT\ln(\Omega)$ . We consider meaningful interactions to have values of  $\Omega \geq 3$  (or  $\leq 1/3$ ), corresponding to  $|\Delta\Delta G^\circ| > 0.6$  kcal/mol.

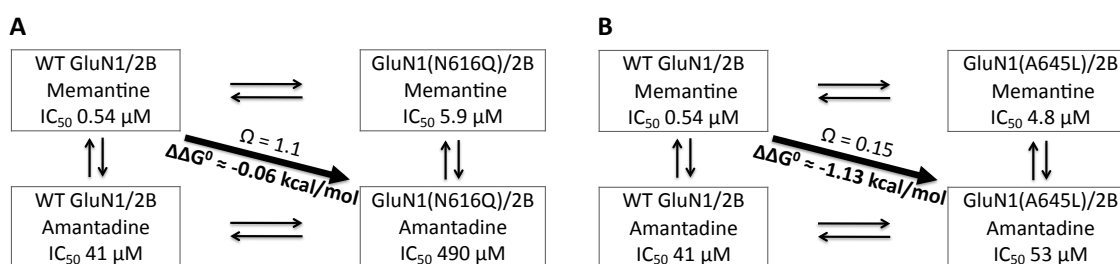


**Figure 3.9.** Examples of mutant-cycle analysis. **(A)** The GluN1(N616Q) mutation showed no coupling at all to the methyl groups of memantine, producing  $\Omega \approx 1$  and  $\Delta\Delta G^\circ \approx 0$  kcal/mol. **(B)** The GluN1(A645L) mutation strongly coupled to the methyl groups as shown by the substantial coupling energy  $\Delta\Delta G^\circ$ .

Memantine and amantadine show similar responses to the GluN1(N616Q) and GluN1(N616D) mutations, indicating that the two drugs block the channel at the same general location and with the same orientation (Figure 3.4). Stated differently, these two mutations, which are thought to probe the ammonium group binding site, show no significant coupling to the memantine/amantadine pair ( $\Delta\Delta G^\circ < 0.4$ ) (Table 3.3), which is a probe of methyl group binding. Therefore, comparison of the IC<sub>50</sub> shifts between the two drugs is a valid strategy for probing the residues that are interacting with the methyl groups of memantine.

**Table 3.3.** Memantine and amantadine IC<sub>50</sub> ± s.e.m., Ω, and ΔΔG° for wild-type and mutant NMDA receptors

NMDA Receptor	Memantine IC <sub>50</sub>		Amantadine IC <sub>50</sub>		Ω <sup>a</sup>	ΔΔG° <sup>b</sup>
	μM	<i>n</i>	μM	<i>n</i>		
Wild type	0.54 ± 0.03	18	41 ± 5.6	6		
<b>GluN1 Mutants</b>						
N616Q	5.9 ± 0.5	6	490 ± 73	10	1.1	-0.06
N616D	14 ± 1.3	7	590 ± 21	5	0.55	0.35
V644T	0.26 ± 0.06	13	44 ± 15	13	2.2	-0.48
V644L	0.26 ± 0.09	15	26 ± 6.5	11	1.3	-0.17
V644N	12 ± 3.2	7	150 ± 27	8	0.16	1.1
A645V	0.60 ± 0.06	9	21 ± 0.8	14	0.46	0.47
A645L	4.8 ± 0.4	9	53 ± 4.4	9	0.15	1.1
A645N	240 ± 16	11	1000 ± 68	11	0.06	1.7
V656N	2.4 ± 0.2	8	94 ± 14	7	0.53	0.38
<b>GluN2B Mutants</b>						
N615D	1.3 ± 0.3	7	300 ± 17	9	3.1	-0.67
N616D	1.0 ± 0.1	6	56 ± 5.3	10	0.74	0.18
A639N	3.6 ± 0.4	10	140 ± 26	11	0.51	0.39
V640N	0.29 ± 0.03	11	12 ± 2.6	8	0.55	0.35
L643N	34 ± 2.7	10	750 ± 130	13	0.29	0.73
A644V	0.41 ± 0.05	14	10. ± 0.7	11	0.33	0.66
A644L	0.29 ± 0.07	12	3.6 ± 0.4	12	0.17	1.0
A644N	90 ± 2.0	9	340 ± 29	10	0.05	1.8

<sup>a</sup> Ω = [(wild-type memantine IC<sub>50</sub>)\*(mutant amantadine IC<sub>50</sub>)]/[wild-type amantadine IC<sub>50</sub>]/(mutant memantine IC<sub>50</sub>).

<sup>b</sup> ΔΔG° = R•T•ln(Ω) where R = 1.987 kcal•mol<sup>-1</sup>•K<sup>-1</sup> and T = 298 K.

The Asp mutation at GluN2B-N615, the residue that is considered to align with GluN1-N616, is the only mutation that affects amantadine binding more than memantine. This observation suggests an asymmetry in the region of the

ammonium group binding site such that the GluN1 subunit plays a more important role in memantine block, in agreement with previous proposals (12, 31).

In GluN1, the V644N and A645N mutations, which displayed a large reduction in the methyl group effect from the wild type (Figure 3.5), produced a substantial  $\Delta\Delta G^\circ$  of 1.1 kcal/mol and 1.7 kcal/mol, respectively, (Table 3.3). A strong interaction between the side chain of the residue A645 and the methyl groups of memantine is indicated here, and the location of this residue relative to the residue GluN1-N616 on our homology model supports this finding (Figure 3.2). This is in an agreement with a previous study based on the SCAM showing that in the GluN1/GluN3 receptor, GluN1-A645 in the TM3 of the GluN1/GluN3 receptor is in a close proximity to the GluN1-N616 site (41). In contrary, the mutation V656N only produced a negligible  $\Delta\Delta G^\circ$  of 0.38 kcal/mol, suggesting that the effect of this mutation was not specific to the methyl groups on memantine.

The A645L mutation in GluN1, which had a significant impact on memantine  $IC_{50}$  but not amantadine  $IC_{50}$  (Figure 3.6), resulted in a significant  $\Delta\Delta G^\circ$  of 1.1 kcal/mol (Table 3.3). Since Leu and Ala are both hydrophobic, this could be considered a steric effect. When the methyl groups of memantine are present, a significant steric clash occurs when Ala is mutated to Leu. With amantadine, however, essentially no effect is seen. The lesser impact of the Val mutation, with  $\Delta\Delta G^\circ$  of 0.47 kcal/mol, is consistent with this analysis. Leu can be considered to be isosteric to Asn, and so the additional perturbation for the Asn mutation ( $\Delta\Delta G^\circ$  1.7 kcal/mol) relative to Leu ( $\Delta\Delta G^\circ$  1.1 kcal/mol) can be

considered a polarity effect. Both results are consistent with the notion that GluN1-A645 contributes to a hydrophobic binding pocket for the methyl groups on memantine.

To probe for contributions to a methyl group binding site by GluN2B, we considered the aligning residues, L643 and A644, as well as the residues A639 and V640 in order to address the possibility of the offset in the TM3 regions between the two subunits (Figure 3.2). Both A639N and V640N mutations resulted in a small perturbation to memantine and amantadine affinities and a negligible  $\Delta\Delta G^\circ$  value, whereas the L643N and A644N mutations produced a considerable effect. While GluN2B(L643N) showed a modest differentiation between memantine and amantadine and a  $\Delta\Delta G^\circ$  value of 0.73 kcal/mole, GluN2B(A644N) produced a large  $\Delta\Delta G^\circ$  value of 1.8 kcal/mol, comparable to what is seen with the GluN1(A645N) mutation. These data suggest that the offset in the TM3 region between GluN1 and GluN2B is minimal, consistent with a study of felbamate, an anticonvulsant drug that is structurally dissimilar to the antagonists studied here (42).

Mutating the residue GluN2B-A644 to Leu and Val produced the trend in  $\Delta\Delta G^\circ$  values that is very much parallel to that seen for the mutations at GluN1-A645. The large, polar residue Asn has the greatest effect; the isosteric but hydrophobic residue Leu has a smaller but still significant effect; the smaller hydrophobic residue Val has a small/negligible effect.

Overall, these results support a model in which the two residues — GluN1-A645 and GluN2-A644 — play similar roles in shaping the memantine

methyl binding site. However, there is an intriguing distinction between the two sites: the A645L mutation on GluN1 increases memantine  $IC_{50}$  and leaves amantadine  $IC_{50}$  unchanged (Figure 3.6), while the opposite is seen for the A644L mutation on GluN2B which shows no change in memantine  $IC_{50}$  and a lower amantadine  $IC_{50}$  than the wild type (Figure 3.8).

We have identified the hydrophobic binding pockets for the two methyl groups on memantine, which are located on the TM3 helices of the NMDA receptor and are formed by the residues A645 and A644 of GluN1 and GluN2B, respectively. Because these alanine residues are conserved in all the GluN2 subunits (GluN2A/B/C/D), it is possible that the methyl group binding pockets are the same for other GluN1/GluN2 receptor subtypes. These alanine residues are located immediately upstream to the SYTANLAAF motif, which has been implicated to play a crucial role in gating of the NMDA receptor (43–45).

Although we performed our experiments in a  $Mg^{2+}$ -free environment, it is worth noting that a decrease in the potencies of both memantine and amantadine has been reported in the presence of physiological concentrations of  $Mg^{2+}$  (46, 47). This observation suggests a competitive behavior between memantine and  $Mg^{2+}$ , consistent with the notion that they share a common blocking location at the tip of the pore loop. The implication is that the primary binding site of memantine, including the methyl group binding pockets, possibly remains unchanged in the system with  $Mg^{2+}$ .

The two methyl groups on memantine are crucial for NMDA receptor blockade, increasing memantine affinity to the open NMDA receptor channel

and making it a much better neuroprotective drug than amantadine. We found that the molecule TMAm, which bears an additional methyl group compared to memantine, is also an antagonist to the NMDA receptor with an affinity between those of memantine and amantadine (Table 3.2). However, the TMAm block exhibited less sensitivity to the Asn mutations at GluN1-A645 or GluN2-A644 and was totally insensitive to the mutations GluN1(N616Q), GluN2(N615D), and GluN2(N616D) in the pore loop (Table 3.2). Altogether, our results suggest that the additional methyl group on TMAm prevents it from binding the receptor at the same location or orientation as memantine and amantadine.

In summary, our results indicate that the primary binding interaction of the methyl groups of memantine is formed by GluN1-A645 and GluN2-A644. Mutation at these residues had a significantly larger effect on memantine block compared to amantadine block. When coupled with the interaction between the ammonium group and GluN1-N616, a fairly precise model of memantine binding can be produced. Furthermore, the study of TMAm reveals that the special property of memantine as an NMDA receptor blocker stems not only from the presence of the additional hydrophobicity gained from the two methyl groups on the amantadine core but also a proper shape-matching to the binding site. Our findings provide further insight into the chemical-scale interaction between the NMDA receptor and memantine, hopefully contributing to efforts to understand the drug's high clinical potential and accelerate the development of other therapeutic NMDA receptor antagonists.

### 3.4 Materials and Methods

#### *NMDAR Clones and Mutagenesis*

The rat GluN1-1a and rat GluN2B cDNA clones were in pAMV vector. Mutant GluN1 and GluN2B subunits were prepared by site-directed mutagenesis using the standard Stratagene QuikChange protocol and verified through sequencing. All cDNA was linearized with NotI, and mRNA was synthesized by in vitro runoff transcription using the T7 mMESSAGE mMACHINE kit (Ambion).

#### *Oocyte Expression*

Stage V–VI *Xenopus laevis* oocytes (Nasco) were injected with 4–75 ng of mRNA in a total volume of 50 nL per oocyte. For some mutant receptors, second injection was necessary to attain sufficient current size, which was given 24 hours after the first injection. Oocytes were incubated in ND96<sup>+</sup> solution for 18 hours to 4 days after initial injection to achieve the optimal current size for the experiments.

#### *Electrophysiological Recordings*

Amantadine was purchased from Aldrich, memantine from Tocris Bioscience. Amantadine was stored as 1M stock solution and memantine as 100 mM stock solution in Millipore water at –80 °C. Glycine and L-glutamic acid

hydrochloride were purchased from Aldrich and were stored at  $-80\text{ }^{\circ}\text{C}$  as 1M and 100 mM in Millipore water, respectively.

Macroscopic current recordings were made in two-electrode voltage-clamp mode using the OpusXpress 6000A (Molecular Devices). Voltage-sensing electrodes had a resistance of 0.3–10 M $\Omega$ , and current-injecting electrodes, 0.3–3 M $\Omega$ ; all were filled with 3 M KCl. Oocytes were evaluated in a  $\text{Mg}^{2+}$  and  $\text{Ca}^{2+}$ -free saline solution (96 mM NaCl, 5 mM HEPES, 2 mM KCl, and 1 mM  $\text{BaCl}_2$ , pH 7.5). The receptors were activated in a  $\text{Mg}^{2+}$ - and  $\text{Ca}^{2+}$ -free solution containing 10  $\mu\text{M}$  glycine and 20  $\mu\text{M}$  glutamate. In the cases of GluN1(A645N) and GluN1(V656N) mutations, 10  $\mu\text{M}$  glycine and 4  $\mu\text{M}$  glutamate were used to activate the receptors to avoid overly saturated glutamate concentration.

To measure memantine  $\text{IC}_{50}$ , the mixture of glutamate and glycine was first applied through pump B. Memantine was then co-applied with the agonists for 50 seconds via a pipette tip, and after that, the agonists were applied again for 80 seconds through pump B. Then cells were later washed for 3 minutes in the  $\text{Mg}^{2+}$ - and  $\text{Ca}^{2+}$ -free ND96 solution. Similar protocol was used with amantadine but with different application durations: 35 seconds of the first agonist application, 30 seconds of amantadine applications, 45 seconds of the second agonist application, and 125 seconds of wash.

Up to eight oocytes were simultaneously voltage-clamped at  $-80\text{ mV}$ , and dose-response relationships were obtained by delivery of various drug concentrations in 1 mL aliquots.

### *Data analyses*

All data were analyzed using the Clampfit 9.0 software (Axon). To determine  $IC_{50}$ , the fraction of block current ( $I/I_{max}$ ) was determined for each test dose of antagonist, where  $I$  is the agonist-activated current measured in the presence of antagonist and  $I_{max}$  is the maximal current response to agonist activation. Then the  $I/I_{max}$  values were averaged for a given antagonist concentration, and the averages were fitted to the Hill equation. To determine  $EC_{50}$ , dose-response data were normalized to the maximal current ( $I_{max} = 1$ ) and averaged.  $EC_{50}$  and Hill coefficient ( $n_H$ ) were determined by fitting averaged, normalized dose-response relations to the Hill equation. All dose-response data were obtained from at least 5 cells and at least two batches of oocytes. Dose responses of individual oocytes were also examined and used to determine outliers.

### 3.5 Supplementary Figures

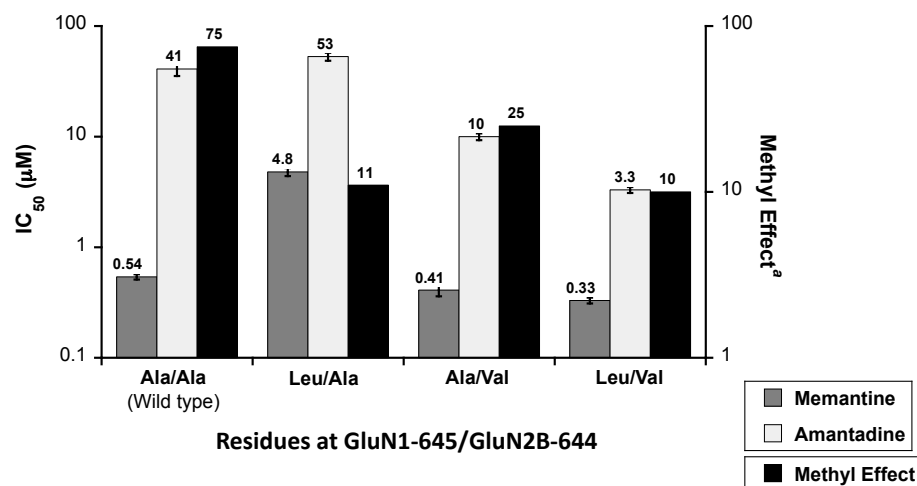


**Figure 3.S1.** Memantine IC<sub>50</sub>, amantadine IC<sub>50</sub>, and the methyl effect for double mutant GluN1(A645L)/2B(A644V) NMDA receptor in comparison with the values from the wild-type and the single-mutant receptors

### 3.6 References

- (1) Dingledine, R.; Borges, K.; Bowie, D.; Traynelis, S. F. The glutamate receptor ion channels. *Pharmacol. Rev.* **1999**, *51*, 7–61.
- (2) Madden, D. R. The structure and function of glutamate receptor ion channels. *Nat. Rev. Neurosci.* **2002**, *3*, 91–101.
- (3) Traynelis, S. F.; Wollmuth, L. P.; McBain, C. J.; Menniti, F. S.; Vance, K. M.; Ogden, K. K.; Hansen, K. B.; Yuan, H.; Myers, S. J.; Dingledine, R. Glutamate receptor ion channels: structure, regulation, and function. *Pharmacol. Rev.* **2010**, *62*, 405–496.
- (4) Moriyoshi, K.; Masu, M.; Ishii, T.; Shigemoto, R.; Mizuno, N.; Nakanishi, S. Molecular cloning and characterization of the rat NMDA receptor. *Nature* **1991**, *354*, 31–37.
- (5) Nakanishi, N.; Axel, R.; Shneider, N. A. Alternative splicing generates functionally distinct N-methyl-D-aspartate receptors. *Proc. Natl. Acad. Sci. U.S.A.* **1992**, *89*, 8552–8556.

- (6) Ascher, P.; Nowak, L. The role of divalent cations in the N-methyl-D-aspartate responses of mouse central neurones in culture. *J. Physiol. (London)* **1988**, *399*, 247–266.
- (7) Kullmann, D. M.; Asztely, F.; Walker, M. C. The role of mammalian ionotropic receptors in synaptic plasticity: LTP, LTD and epilepsy. *Cell. Mol. Life Sci.* **2000**, *57*, 1551–1561.
- (8) Liu, L.; Wong, T. P.; Pozza, M. F.; Lingenhoehl, K.; Wang, Y.; Sheng, M.; Auberson, Y. P.; Wang, Y. T. Role of NMDA receptor subtypes in governing the direction of hippocampal synaptic plasticity. *Science* **2004**, *304*, 1021–1024.
- (9) Hollmann, M.; Heinemann, S. Cloned glutamate receptors. *Annu. Rev. Neurosci.* **1994**, *17*, 31–108.
- (10) Malinow, R.; Mainen, Z. F.; Hayashi, Y. LTP mechanisms: from silence to four-lane traffic. *Curr. Opin. Neurobiol.* **2000**, *10*, 352–357.
- (11) Cull-Candy, S.; Brickley, S.; Farrant, M. NMDA receptor subunits: diversity, development and disease. *Curr. Opin. Neurobiol.* **2001**, *11*, 327–335.
- (12) Chen, H.-S. V.; Lipton, S. A. The chemical biology of clinically tolerated NMDA receptor antagonists. *J. Neurochem.* **2006**, *97*, 1611–1626.
- (13) Witt, A.; Macdonald, N.; Kirkpatrick, P. Memantine hydrochloride. *Nat. Rev. Drug Discovery* **2004**, *3*, 109–110.
- (14) Parsons, C. G.; Stöffler, A.; Danysz, W. Memantine: a NMDA receptor antagonist that improves memory by restoration of homeostasis in the glutamatergic system--too little activation is bad, too much is even worse. *Neuropharmacology* **2007**, *53*, 699–723.
- (15) Wilkinson, D. A review of the effects of memantine on clinical progression in Alzheimer's disease. *Int. J. Geriatr. Psychiatry* **2012**, *27*, 769–776.
- (16) Bormann, J. Memantine is a potent blocker of N-methyl-D-aspartate (NMDA) receptor channels. *Eur. J. Pharmacol.* **1989**, *166*, 591–592.
- (17) Chen, H. S.; Pellegrini, J. W.; Aggarwal, S. K.; Lei, S. Z.; Warach, S.; Jensen, F. E.; Lipton, S. A. Open-channel block of N-methyl-D-aspartate (NMDA) responses by memantine: therapeutic advantage against NMDA receptor-mediated neurotoxicity. *J. Neurosci.* **1992**, *12*, 4427–4436.
- (18) La Spada, A. Memantine strikes the perfect balance. *Nat. Med.* **2009**, *15*, 1355–1356.
- (19) Johnson, J. W.; Kotermanski, S. E. Mechanism of action of memantine. *Curr. Opin. Pharmacol.* **2006**, *6*, 61–67.

- (20) Kuner, T.; Seeburg, P. H.; Guy, H. R. A common architecture for K<sup>+</sup> channels and ionotropic glutamate receptors? *Trends Neurosci.* **2003**, *26*, 27–32.
- (21) Wollmuth, L. P.; Sobolevsky, A. I. Structure and gating of the glutamate receptor ion channel. *Trends Neurosci.* **2004**, *27*, 321–328.
- (22) Sobolevsky, A. I.; Rosconi, M. P.; Gouaux, E. X-ray structure, symmetry and mechanism of an AMPA-subtype glutamate receptor. *Nature* **2009**, *462*, 745–756.
- (23) Long, S. B.; Tao, X.; Campbell, E. B.; Mackinnon, R. Atomic structure of a voltage-dependent K<sup>+</sup> channel in a lipid membrane-like environment. *Nature* **2007**, *450*, 376.
- (24) Kornhuber, J.; Bormann, J.; Hübers, M.; Rusche, K.; Riederer, P. Effects of the 1-amino-adamantanes at the MK-801-binding site of the NMDA-receptor-gated ion channel: a human postmortem brain study. *Eur. J. Pharmacol.* **1991**, *206*, 297–300.
- (25) Lupp, A.; Lücking, C. H.; Koch, R.; Jackisch, R.; Feuerstein, T. J. Inhibitory effects of the antiparkinsonian drugs memantine and amantadine on N-methyl-D-aspartate-evoked acetylcholine release in the rabbit caudate nucleus in vitro. *J. Pharmacol. Exp. Ther.* **1992**, *263*, 717–724.
- (26) Parsons, C. G.; Quack, G.; Bresink, I.; Baran, L.; Przegalinski, E.; Kostowski, W.; Krzascik, P.; Hartmann, S.; Danysz, W. Comparison of the potency, kinetics and voltage-dependency of a series of uncompetitive NMDA receptor antagonists in vitro with anticonvulsive and motor impairment activity in vivo. *Neuropharmacology* **1995**, *34*, 1239–1258.
- (27) Blanpied, T. A.; Boeckman, F. A.; Aizenman, E.; Johnson, J. W. Trapping channel block of NMDA-activated responses by amantadine and memantine. *J. Neurophysiol.* **1997**, *77*, 309–323.
- (28) Blanpied, T. A.; Clarke, R. J.; Johnson, J. W. Amantadine inhibits NMDA receptors by accelerating channel closure during channel block. *J. Neurosci.* **2005**, *25*, 3312–3322.
- (29) Antonov, S. M.; Johnson, J. W. Voltage-dependent interaction of open-channel blocking molecules with gating of NMDA receptors in rat cortical neurons. *J. Physiol. (London)* **1996**, *493 ( Pt 2)*, 425–445.
- (30) Sobolevsky, A. I.; Koshelev, S. G.; Khodorov, B. I. Interaction of memantine and amantadine with agonist-unbound NMDA-receptor channels in acutely isolated rat hippocampal neurons. *J. Physiol. (London)* **1998**, *512 ( Pt 1)*, 47–60.

- (31) Chen, H.-S. V.; Lipton, S. A. Pharmacological implications of two distinct mechanisms of interaction of memantine with N-methyl-D-aspartate-gated channels. *J. Pharmacol. Exp. Ther.* **2005**, *314*, 961–971.
- (32) Sobolevsky, A. I.; Prodromou, M. L.; Yelshansky, M. V.; Wollmuth, L. P. Subunit-specific contribution of pore-forming domains to NMDA receptor channel structure and gating. *J. Gen. Physiol.* **2007**, *129*, 509–525.
- (33) Sobolevsky, A. I.; Rooney, L.; Wollmuth, L. P. Staggering of subunits in NMDAR channels. *Biophys. J.* **2002**, *83*, 3304–3314.
- (34) Lipton, S. A. Paradigm shift in neuroprotection by NMDA receptor blockade: Memantine and beyond. *Nat. Rev. Drug Discovery* **2006**, *5*, 160–170.
- (35) Okamoto, S.-I.; Pouladi, M. A.; Talantova, M.; Yao, D.; Xia, P.; Ehrnhoefer, D. E.; Zaidi, R.; Clemente, A.; Kaul, M.; Graham, R. K.; Zhang, D.; Vincent Chen, H.-S.; Tong, G.; Hayden, M. R.; Lipton, S. A. Balance between synaptic versus extrasynaptic NMDA receptor activity influences inclusions and neurotoxicity of mutant huntingtin. *Nat. Med.* **2009**, *15*, 1407–1413.
- (36) Parsons, C. G.; Gillling, K. E.; Jatzke, C. Memantine does not show intracellular block of the NMDA receptor channel. *Eur. J. Pharmacol.* **2008**, *587*, 99–103.
- (37) Kashiwagi, K.; Masuko, T.; Nguyen, C. D.; Kuno, T.; Tanaka, I.; Igarashi, K.; Williams, K. Channel blockers acting at N-methyl-D-aspartate receptors: differential effects of mutations in the vestibule and ion channel pore. *Mol. Pharmacol.* **2002**, *61*, 533–545.
- (38) Bresink, I.; Benke, T. A.; Collett, V. J.; Seal, A. J.; Parsons, C. G.; Henley, J. M.; Collingridge, G. L. Effects of memantine on recombinant rat NMDA receptors expressed in HEK 293 cells. *Br. J. Pharmacol.* **1996**, *119*, 195–204.
- (39) Bolshakov, K. V.; Gmiro, V. E.; Tikhonov, D. B.; Magazanik, L. G. Determinants of trapping block of N-methyl-D-aspartate receptor channels. *J. Neurochem.* **2003**, *87*, 56–65.
- (40) Mealing, G. A.; Lanthorn, T. H.; Small, D. L.; Murray, R. J.; Mattes, K. C.; Comas, T. M.; Morley, P. Structural modifications to an N-methyl-D-aspartate receptor antagonist result in large differences in trapping block. *J. Pharmacol. Exp. Ther.* **2001**, *297*, 906–914.
- (41) Wada, A.; Takahashi, H.; Lipton, S. A.; Chen, H.-S. V. NR3A modulates the outer vestibule of the “NMDA” receptor channel. *J. Neurosci.* **2006**, *26*, 13156–13166.
- (42) Chang, H.-R.; Kuo, C.-C. Molecular determinants of the anticonvulsant felbamate binding site in the N-methyl-D-aspartate receptor. *J. Med. Chem.* **2008**, *51*, 1534–1545.

- (43) Chang, H.-R.; Kuo, C.-C. The activation gate and gating mechanism of the NMDA receptor. *J. Neurosci.* **2008**, *28*, 1546–1556.
- (44) Yuan, H.; Erreger, K.; Dravid, S. M.; Traynelis, S. F. Conserved structural and functional control of N-methyl-D-aspartate receptor gating by transmembrane domain M3. *J. Biol. Chem.* **2005**, *280*, 29708–29716.
- (45) Blanke, M. L.; VanDongen, A. M. J. The NR1 M3 domain mediates allosteric coupling in the N-methyl-D-aspartate receptor. *Mol. Pharmacol.* **2008**, *74*, 454–465.
- (46) Otton, H. J.; Mclean, A. L.; Pannozzo, M. A.; Davies, C. H.; Wyllie, D. J. A. Quantification of the Mg<sup>2+</sup>-induced potency shift of amantadine and memantine voltage-dependent block in human recombinant GluN1/GluN2A NMDARs. *Neuropharmacology* **2011**, *60*, 388–396.
- (47) Kotermanski, S. E.; Johnson, J. W. Mg<sup>2+</sup> Imparts NMDA Receptor Subtype Selectivity to the Alzheimer's Drug Memantine. *J. Neurosci.* **2009**, *29*, 2774–2779.